Size-dependent surface-plasmon-enhanced photoluminescence from silver nanoparticles embedded in silica

Oleg A. Yeshchenko,[1] Igor M. Dmitruk,[1] Alexandr A. Alexeenko,[2] Mykhaylo Yu. Losytskyy,[1] Andriy V. Kotko,[3] and Anatoliy O. Pinchuk[4]

[1]*Department of Physics, National Taras Shevchenko Kyiv University, 2/1 Akademik Glushkov Prosp., 03127 Kyiv, Ukraine*

[2]*Laboratory of Technical Ceramics and Silicates, Gomel State Technical University, 48 October Prosp., 246746 Gomel, Belarus*

[3]*I. M. Frantsevich Institute for Problems of Materials Science, 3 Krzhizhanovsky Str., 03680 Kyiv, Ukraine*

[4]*Department of Physics and Energy Sciences, University of Colorado at Colorado Springs, 1420 Austin Bluffs Pkwy, Colorado Springs, Colorado 80933, USA*

The size dependence of the photoluminescence spectra from silver nanoparticles embedded in a silica host medium was observed. The quantum yield of the photoluminescence increased when the size of the nanoparticles was decreased. The quantum yield for 8 nm silver nanoparticle was estimated to be on the order of 10^{-2} which is 10^8 times higher than the one observed for bulk silver. The two photoluminescence bands observed from silver nanoparticles were rationalized as the radiative electron interband transitions and radiative decay of the surface plasmons in silver nanoparticles. The strong local electric field induced by the surface-plasmon resonance in silver nanoparticles enhances the exciting and emitted photons and increases the quantum yield of the photoluminescence.

PACS number(s): 78.67.Bf, 78.55.−m, 73.22.Lp, 78.68.+m

I. INTRODUCTION

Noble metal nanoparticles exhibit unique optical properties such as resonant absorption and scattering of light, not found in bulk counterparts.[1,2] Collective coherent excitations of the free electrons in the conduction band are responsible for the strong absorption and scattering of the light by the particles.[1] These coherent oscillations also known as surface plasmon resonance (SPR) lead to an enhanced local electric field close to the surface of the particles.[1–4] The wavelength and width of the SPR band depend on the size, morphology, spatial orientation, and optical constants of the particles and the embedding medium.[2] The strong local electric field in the vicinity of the nanoparticles, sometimes referred to as the "hot spots," can be used in surface enhanced spectroscopy such as surface-enhanced Raman scattering (SERS),[5] surface-enhanced infrared absorption (SEIRA),[6] surface-enhanced fluorescence,[7] etc. While these methods received considerable experimental and theoretical attention,[6,8–10] the luminescence from noble metal nanoparticles has been studied very sparsely,[11,12] partly because of a very low probability of the corresponding radiative transitions.[13–15] In contrast, the luminescence from bulk and nanostructured semiconductors [quantum dots (QD)] has been extensively studied and well understood in terms of a radiative transition defined by the selection rules across the band gap between the conduction and valence bands. Since metals do not have a forbidden energy gap between occupied and unoccupied states in the conduction band, the excited electron can recombine nonradiatively with the hole and this leads to a very low probability of the radiative transition and luminescence process.[13–15] The photoluminescence (PL) from bulk silver,[16] gold, and copper[17] was experimentally observed near the interband absorption edge of the corresponding bulk metal and was attributed to the direct radiative interband recombination of the conduction *sp*-band electrons with holes in the valence *d*

band that have been scattered to momentum states less than the Fermi momentum. The efficiency (quantum yield) of the photoluminescence from bulk noble metals was found to be at the order of 10^{-10}.

The PL from noble metal nanoparticles was reported for gold,[18,19] copper,[20,21] and silver[11,22] nanoparticles. All these measurements revealed the maximum of the PL band close to the interband absorption edge and thus the PL was attributed to the interband radiative transitions.[11,18–22] The PL was observed only from nanoparticles smaller than 20 nm in diameter and from nanorods with a high aspect ratio, which suggests a strong size and morphology dependence of the PL spectra. When the size of the particles decreased, the intensity of the PL increased indicating a strong influence of the surface the nanoparticles on the PL spectra.

The strong local electric field close to the surface of the particles enhances the Raman scattering from molecules functionalized on its surface (SERS) (Refs. 23 and 24) and luminescence from molecules functionalized on the surface of the particles or close to a rough metal surface.[25–27] This suggests that the strong local electric field induced by the SPR excitation in the particle can also enhance the quantum yield of the photoluminescence from the particles. The theory of local enhanced electric field[28] was developed to describe the nonlinear second harmonic generation and Raman scattering by rough metal surfaces. An extension of the theory was developed for noninteracting hemispherical metal particles on a surface.[29] SPR excitations can easily decay through nonradiative electron-phonon scattering. However, there is a probability of radiative decay of SPR excitations which may contribute to the photoluminesce from metal nanoparticles.[11,22]

In this paper, we present the experimental PL spectra from spherical silver nanoparticles in the size range from 8 to 30 nm embedded in a silica host medium. The PL spectra reveal two bands corresponding to interband transitions from elec-
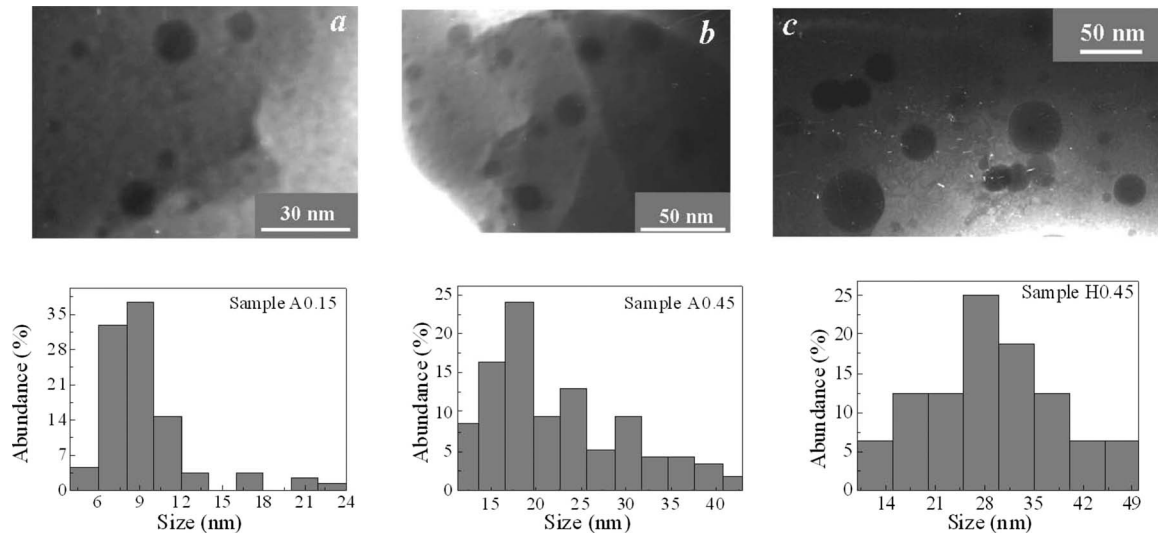
FIG. 1. TEM images with corresponding size distribution histograms of silver nanoparticles in silica glass for samples A0.15 (a) and A0.45 (b) annealed in air and H0.45 (c) annealed in hydrogen.

tron states in the conduction *sp* band to holes states in the valence *d* band and radiative decays of SPR in Ag nanoparticles. The intensity of PL spectra increases with the decrease in the nanoparticle size indicating the enhancement of the PL efficiency. The quantum yield estimated for 8 nm Ag nanoparticles was more than eight orders of magnitude higher than the one for bulk silver. The calculations of the theoretical PL spectra of silver nanoparticles were performed using the model of local-field enhancement.[29] The calculations are in good agreement with the experimental results.

In the next section we describe the experimental procedures of the diffuse reflectance and PL spectroscopy and details of the nanoparticles preparation. Section III outlines the experimental results and presents the theory of the local-field enhancement followed by the discussion and conclusions.

II. EXPERIMENTS

Silver nanoparticles embedded in a SiO_2 host were synthesized according the procedure described in literature.[20,30,31] Porous silica matrices (obtained by transformation to monolithic glasses) were produced using a modified conventional sol-gel technique based on hydrolysis of tetraethoxysilane (TEOS) with doping followed by a chemical transformation of the dopants in air or controlled gaseous medium. A precursor sol was prepared by mixing of TEOS, water, and alcohol with the acid catalysts HNO_3 or HCl. Silica powder with particle size about 5–15 nm (the specific surface area is 380 ± 30 m^2/g) was added to the sol followed by ultrasonication in order to prevent a large volume contraction during drying. The next gelation step resulted in the formation of gels with a desired shape. Porous materials (xerogels) were obtained after the gels were dried at room temperature under controlled humidity. The porosity of SiO_2 matrices was controlled by annealing the samples in air at the temperature of 600 °C during 1 h. The heating process resulted in visible variations of the density and specific surface area. Silver doping was performed by immersion of xe-

rogels into $AgNO_3$ alcohol solution during 24 h. We used the $AgNO_3$ alcohol solutions with three concentrations: 0.15 mmol $(AgNO_3)$/50 ml (alcohol), 0.30 mmol/50 ml, and 0.45 mmol/50 ml. Then, the silver doped samples were dried in air at 40 °C during 24 h. Further processing of the Ag-doped xerogels was done in two different ways: (1) annealing in air with gradual increase of the temperature from 20 °C to 1200 °C (annealing time at 1200 °C: 5 min); (2) the same procedure but performed in hydrogen atmosphere. The annealing resulted in reduction in Ag(I) to Ag(0) and then in aggregation in the form of Ag nanoparticles. The samples obtained by annealing in air had low-optical density and were noncolored (labeled hereafter as samples A) and the samples obtained using annealing in hydrogen atmosphere had a higher optical density and had yellow color (labeled as samples H). We fabricated six samples: A0.15, A0.30, A0.45 and H0.15, H0.30, H0.45 corresponding to different concentrations of $AgNO_3$ in alcohol solution mentioned above.

The transmission electron microscopy (TEM) of fabricated Ag/SiO_2 glass samples was made to determine the size and shape distribution of nanoparticles. TEM characterization was performed using JEOL 100CX electron microscope operating at 100 kV. The TEM measurements were performed for the powdered pieces of Ag/SiO_2 glass samples. The TEM images were taken from the edge of the fragments of powder, since only the edge can be transmitted by the electron beam. Therefore, the different areas of obtained TEM images have the different thickness and contrast. The size distributions of the silver nanoparticles in different studied samples were obtained by the analysis of 40–140 nanoparticles depending on the sample. Figure 1 shows some examples of the TEM images of typical samples A0.15, A0.45, and H0.45 with the corresponding histograms showing the size distribution of Ag nanoparticles. The silver nanoparticles have the spherical shape and the diameter of the particles was estimated for different samples: sample A0.15 ($\langle d \rangle$ =8 nm with standard deviation σ_d=2.7 nm), A0.30 ($\langle d \rangle$ =11 nm with σ_d=4.1 nm), A0.45 ($\langle d \rangle$=17 nm with σ_d

=6.2 nm), H0.15 ($\langle d \rangle$=22 nm with σ_d=9.1 nm), H0.30 ($\langle d \rangle$=26 nm with σ_d=10.4 nm), and H0.45 ($\langle d \rangle$=30 nm with σ_d=13.4 nm). The TEM results indicate a large separation between nanoparticles, so that the electrodynamic coupling does not affect their optical spectra. One can see that the increase in the concentration of salt $AgNO_3$ in initial xerogel and the annealing in hydrogen leads to the increase in the size of silver nanoparticles.

A tungsten-halogen incandescent lamp was used as a light source for the absorption and diffuses reflectance (DR) measurements. DR spectra were recorded in the near backscattering geometry where the angle between the exciting and reflected beams was about 15°. The single spectrometer MDR-3 was used for the registration of the DR spectra. The PL and the excitation spectra of Ag/SiO_2 glass nanocomposites were measured by Cary Eclipse (Varian Inc.) fluorescence spectrophotometer. The photoluminescence was excited by a single monochromatic line (spectral half width of 5 nm) cut from the continuum emission spectrum of pulse Xe lamp. The tuning of exciting wavelength was made in spectral range of 220–400 nm. All measurements were performed at room temperature. The quantum yield of PL from silver nanoparticles was measured by comparing of their photoluminescence intensity with one of anthracene film with known quantum yield of 0.9.

III. RESULTS AND DISCUSSION

A. Diffuse reflectance spectra of Ag/SiO_2 nanocomposites

Noble metal nanoparticles exhibit a strong resonant extinction (absorption plus scattering) of the light in the visible and infrared (IR) frequency range caused by the SPR collective coherent excitations. In this subsection, we outline the experimental and theoretical results on the scattering efficiency of silver nanoparticles embedded in a SiO_2 host medium. Since the measurements of the absorption spectra of silver nanoparticles were hindered by the strong scattering of the light by the host medium, we present the experimental DR spectra of the composites in the near backscattering geometry (see Sec. II). Figure 2 shows the DR spectra of Ag/SiO_2 samples containing silver nanoparticles of different sizes. The DR spectra reveal the P_s band with the maximum around 400 nm associated with the excitation of the SPR of silver nanoparticles, see Fig. 2. The SPR wavelength shifts from 395 nm for nanoparticles of 30 nm size to 416 nm for smaller nanoparticles having the size 8 nm. In addition, we observe broadening of the peak as the size of the nanoparticles decreases.

The density of silver nanoparticles embedded in the SiO_2 host is low, therefore we can neglect the electrodynamic interaction between the particles and use the Mie theory to calculate the scattering efficiency of light by the composite.[1,2] The optical constants for bulk silver were taken from the literature.[32] When the size of the particles becomes smaller than the mean-free path of the electrons in bulk metal, the scattering of the electrons by the surface of the particles leads to the broadening of the SPR band and is referred as the internal size effect.[1] The complex dielectric function of the silver nanoparticles is then modified to take
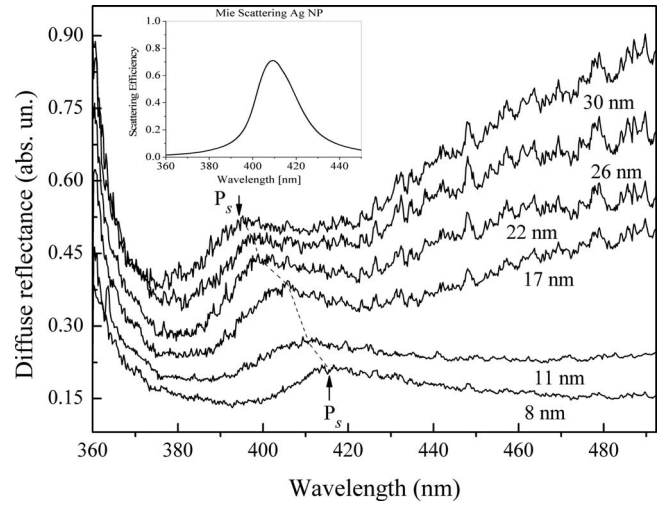
FIG. 2. The diffuse reflectance spectra of Ag/SiO_2 nanocomposite glasses containing the silver nanoparticles with various mean sizes. Inset presents the scattering spectrum of silver nanoparticles in silica matrix calculated by Mie theory.

into account the surface and interface damping of the SPR excitation[1,33]

$$\varepsilon(\omega,R) = \varepsilon'(\omega) + \varepsilon''(\omega)\left[1 + A\frac{l_\infty}{R}\right], \qquad (1)$$

where $\varepsilon'(\omega)$ and $\varepsilon''(\omega)$ are the real and imaginary parts of dielectric function of bulk silver, A is the constant which accounts for both surface and interface scattering effects,[1,33,34] l_∞=55.6 nm is the bulk scattering length for the conduction electrons. The later was calculated assuming the Drude model[35] for the conduction electrons $l_\infty = v_F \tau$, where the Fermi velocity for bulk silver v_F=1.39×10^8 cm/sec and the relaxation time for bulk silver at room temperature T =297 K, τ=4.0×10^{-14} sec. Theoretical spectrum of a composite consisting of well separated silver spherical nanoparticles embedded in a silica host medium is shown in Fig. 2 as an inset. The size of the particles was assumed to be 30 nm and in addition we took into account the size distribution of the particles as estimated from TEM measurements, see Sec. II. The maximum of the scattering intensity corresponds to the SPR excitation wavelength of silver nanoparticles, λ_{SPR} =410 nm, which is in agreement with the experimental results shown in Fig. 2. Thus, we conclude that the maximum in the DR experimental spectra shown in Fig. 2 is caused by the excitation of the SPR in silver nanoparticles. The experimentally observed SPR wavelength red shifts as the nanoparticle size decreases. The red shift might be caused either the spill-out effect[1] or by the presence of the oxide shell around the silver core. The silver oxide shell would have a higher index of refraction than the host silica matrix and would lead to the red shift of the SPR band as observed experimentally. However, this hypothesis deserves a detailed discussion and will be addressed in more details in an upcoming publication.

$\lambda_{exc} = 250$ nm

(a)

$\lambda_{exc} = 250$ nm

(b)
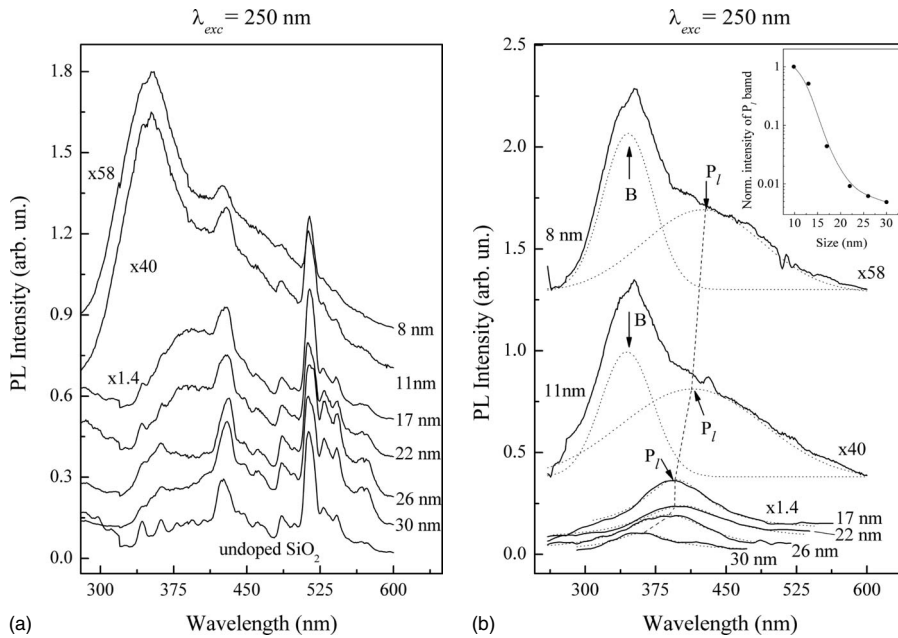
FIG. 3. (a) Photoluminescence spectra of Ag/SiO₂ nanocomposite glasses containing the silver nanoparticles of various sizes and pure silica glass. (b) The same PL spectra but after subtraction of the spectrum of pure silica matrix. *B* and P$_l$ bands originate from interband radiative transitions and radiative decay of surface plasmons in silver nanoparticles correspondingly. Inset demonstrates the size dependence of normalized intensity of P$_l$ band. Excitation wavelength is 250 nm. Note $(\times C)$ means that the intensity of corresponding spectrum must be multiplied by a factor C.

B. Photoluminescence from silver nanoparticles

Figure 3(a) shows experimental PL spectra of Ag/SiO₂ composites containing nanoparticles of several different average sizes. In addition, the PL of a pure annealed silica sample prepared from xerogel without silver dopant (AgNO₃) is shown in Fig. 3(a). To separate the PL spectra from silver nanoparticles and those of the silica host, the later was subtracted from the original spectra of the composites shown in Fig. 3(a). The results are shown in Fig. 3(b) as the PL from silver nanoparticles. We can identify two bands denoted as P_l and B in the PL spectra of silver nanoparticles, Fig. 3(b). Both bands can be rationalized either by the PL from silver nanoparticles or by the PL from their oxides or ions, which might be present in the samples annealed in the air, but we rule out the PL from silver oxides and ions later in the discussion.

Let us now analyze the PL spectra from silver nanoparticles. The band denoted as B is observed only in the spectra of the samples containing the smallest Ag nanoparticles (8 and 11 nm) and is absent in the samples with larger particles. Its maximum is at 345 nm, that is very close to the maximum (3.75 eV or 330 nm) of PL band of bulk silver.[15,16] The PL band was experimentally observed for the first time for bulk silver[16] with the maximum at 330 nm and was attributed to direct radiative interband recombination of the conduction *sp*-band electrons with holes in the valence *d* band that have been scattered to momentum states less than the Fermi momentum.[15] The maximum of the band was close to the interband absorption edge of bulk silver[15] (3.2 eV or 388 nm). A similar PL band with its maximum around 330 nm was observed from silver nanoparticles.[11,36] Since the PL spectra in our experiments reveal the maximum which is close to those PL maxima mentioned above, we attribute the B band (345 nm) to the interband $sp \rightarrow d$ radiative transitions. The red shift of the B band relative to the PL band from bulk silver is probably caused by the coupling of the incoming (exciting) and outgoing (emitted) photons with SPR as discussed below.

The second PL band denoted as P_l was observed in the wavelength range of SPR excitation (P$_s$ band in DR spectra). Both P_l and P$_s$ bands are red shifted when the size of the particles decreases [Figs. 2 and 3(b)]. Based on these observations, we attribute the P_l band to radiative decay of SPR excited in silver nanoparticles. The radiative decay of the SPR excitations in silver nanoparticles and nanorods was observed experimentally and reported in the literature.[11,22,37]

As we already mentioned in the introduction, metals do not have a band gap and the probability of the radiative transitions of the electronic excitations down to the ground state is exceedingly low.[13–15,17] Indeed, the quantum yield of the PL from bulk noble metals was estimated on the order of 10^{-10}. Let us note the strong size dependences of intensities of the PL of both B and P_l bands. While the B band is observed only for the smallest (8 and 11 nm) nanoparticles, the intensity of the P_l band decreases significantly as the size of the particles increases as shown in the inset in Fig. 3(b). This strong size dependence of the PL bands gives us some hints as to why the quantum yield of the PL from silver nanoparticles is considerably higher than the one observed from bulk metals. The quantum yield of the interband PL (B band) from silver nanoparticles (8 and 11 nm) using anthracene films with known quantum yield (0.9) was estimated to be 1.2×10^{-2} for 8 nm and 4.6×10^{-3}—for 11 nm silver nanoparticles. This quantum yield is nearly 7–8 orders of magnitude higher than the one observed for bulk noble metals (10^{-10}). Thus, the PL from silver nanoparticles with size about 10 nm is enhanced by eight orders of magnitude. Below we prove that this enhancement is caused by the strong local electric field due to SPR excitation in silver nanoparticles, which results in the enhancement of the electric fields of incoming (exciting) and outgoing (emitted) photons by the SPR. Note that the maximum of the enhancement is observed for silver nanoparticles with size of about 10 nm, which is in agreement with theoretical calculations of the local-field enhancement near surface of silver nanoparticle[38] and reported data on SERS (Refs. 23, 24, and 39) and

luminescence[25] in the molecules adsorbed on the rough silver surfaces and on the surface of silver nanoparticles.

C. Calculations of SPR enhanced PL from silver nanoparticles

The theory of local enhanced electric field by rough surfaces was successfully applied to describe their linear and nonlinear optical properties.[28] Boyd *et al.*[29] developed a theory for a system of noninteracting hemispheres on a metal substrate and showed that the PL intensity depends on the aspect ratio of the particles. The electric fields of incoming (exciting) and outgoing (emitted) photons are enhanced via coupling to the SP resonance.[29] We use this theory to validate the hypothesis of the SPR enhanced PL in our experiments. According to the theory, the local electric field inside a particle is enhanced by the factor known as the local-field correction factor

$$L(\omega) = \frac{D^{-1}}{\varepsilon(\omega) - 1 + D^{-1}\left\{1 + i\frac{4\pi^2 V[1 - \varepsilon(\omega)]}{3\lambda^3}\right\}}, \quad (2)$$

where D is the depolarization factor ($D = 1/3$ for spherical particle), $\varepsilon(\omega)$ is the frequency-dependent complex dielectric function of the metal, λ is the light wavelength. The power of single-photon luminescence $P(\omega_l)$ from a metal nanoparticle excited with a photon of the energy $\hbar\omega_{exc}$ is given by

$$P(\omega_l) = 2^4 \beta(\omega_l)|E_0|^2 V |L^2(\omega_{exc})L^2(\omega_l)|, \quad (3)$$

where E_0 is the incident electric field, $\beta(\omega_l)$ is the function, which includes the intrinsic luminescence spectrum of bulk metal, V is the volume of the particle. The PL spectra from silver nanoparticles can be calculated using the local enhancement factor for the exciting $L(\omega_{exc})$ and emitted $L(\omega_l)$ photons.

The theoretical PL spectra from silver nanoparticles $P(\omega_l)/|E_0|^2$ for different sizes of the nanoparticles are shown in Fig. 4. The complex dielectric function for metal nanoparticles was taken from the literature[32] and modified by including the internal size effect[34] using Eq. (1). The theoretical spectra reflect qualitatively the two bands structure of the PL spectra observed experimentally, Fig. 3(b). The high-energy band with the maximum around 335 nm, denoted as the *B* band, is rationalized above to the interband radiative transitions in bulk silver. This maximum is accounted for by $\beta(\omega_l)$ factor in Eq. (3), which stands for the bulk contribution to the PL spectra. The intensity of the *B* band changes synchronously with the intensity of SP's P_l band, which, we believe, is caused by the coupling of the incoming and outgoing photons to the SPR excitation. The coupling to the SPR excitation results in the enhancement of interband luminescence band.

The second (low energy) band is the one caused by the radiative decay of the SPR excitation, namely the P_l band. The maximum of the P_l band is around 400 nm, Fig. 4. The size dependence of the PL spectra reflects two distinct size effects relative the SPR excitation in silver nanoparticles. As the size of the nanoparticles becomes larger than 30 nm, the radiative damping effect causes the decrease in the local
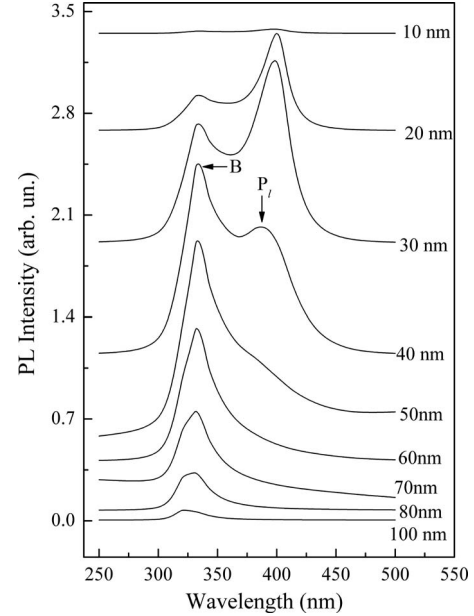
FIG. 4. Calculated photoluminescence spectra of silver nanoparticles of various sizes.

electric field inside the particles. This leads to a decrease in the PL spectra since the enhancement of the PL due to the coupling with the SPR excitation is damped by the radiative losses. On the other hand, when the size of the particle becomes smaller than the mean-free path of the conduction electrons inside the particles, the scattering from the surface and interface damping causes an analogous damping of the SPR excitation and consequently leads to a decrease in the PL intensity, Fig. 4. These two effects—radiative damping and internal size effect lead to a maximum in the PL spectra when the size of the particles becomes close to 30 nm, Fig. 4. The experimental PL spectra are broadened due to a large size distribution of the silver nanoparticles and thus due to the shift of the SPR wavelength, which depends on the size of the particles.[1,2] In addition to the capture of the size effect, the model provides the correct blue shift of the P_l band due to the coupling of the two bands, Fig. 4. As the size of the nanoparticles increases, the maximum of the P_l band shifts to the blue side of the spectrum as observed experimentally, Fig. 3(b).

The theory of the enhanced PL from metal nanoparticles[29] provides the formula to calculate the enhancement factor of the PL from nanoparticle relative to that of PL from smooth planar surface. According to this theory for the power of one-photon PL from bulk metal is given by[29]

$$P_b(\omega_l) = \beta(\omega_l)|E_0|^2 S z_0(\omega_{exc}, \omega_l)|L_b^2(\omega_{exc})L_b^2(\omega_l)|, \quad (4)$$

where $z_0(\omega_{exc}, \omega_l) = [\alpha(\omega_{exc}) + \alpha(\omega_l)]^{-1}$ is the effective absorption depth, $\alpha(\omega)$ is the absorption coefficient, S is the illuminated area, $L_b(\omega_{exc})$ and $L_b(\omega_l)$ are the Fresnel coefficients for planar surface of bulk metal for exciting and emitted photons correspondingly. The Fresnel coefficients are given by
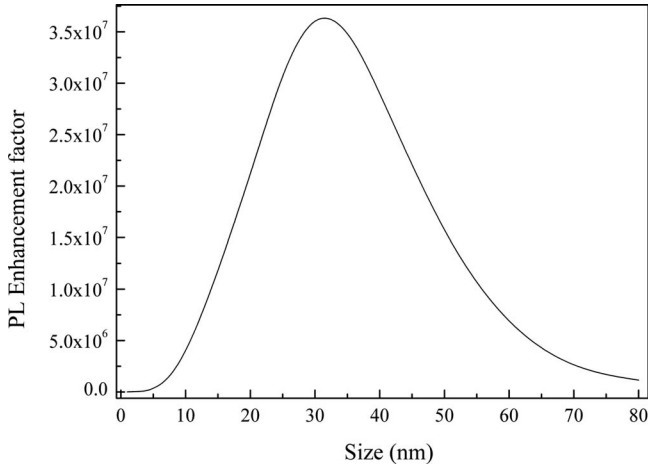
FIG. 5. Calculated size dependence of PL enhancement factor for silver nanoparticles.

$$L_b(\omega) = \frac{2\cos\theta}{\varepsilon^{1/2}(\omega)\cos\theta_0 + \cos\theta}, \tag{5}$$

where θ_0 and θ are the incidence and refraction angles correspondingly. To compare quantitatively the efficiencies of PL from nanoparticle and bulk metal we evaluated S as the cross-section of the nanoparticle ($S = \pi d^2/4$). Thus, the enhancement factor η obtained from Eqs. (3) and (4) can be written as

$$\eta = \frac{P}{P_b} = 2^4 \frac{2d}{3z_0} \frac{|L^2(\omega_{exc})L^2(\omega_l)|}{|L_b^2(\omega_{exc})L_b^2(\omega_l)|}. \tag{6}$$

With the excitation wavelength $\lambda_{exc} = 250$ nm and optical constants for bulk silver taken from the literature,[32] and considering the case of normal incidence of light to surface of bulk metal ($\theta_0 = 0^0$) we calculated the size dependence of PL enhancement factor, see Fig. 5. The highest enhancement of the PL (3.5×10^7 times) from silver nanoparticles is expected for 30 nm silver nanoparticles. The theoretical en-

hancement factor is in good agreement with the experimental one ($1.2 \times 10^{-2}/10^{-10} = 1.2 \times 10^8$—for 8 nm nanoparticles and $4.6 \times 10^{-3}/10^{-10} = 4.6 \times 10^7$—for 11 nm nanoparticles). This agreement proves that the enhancement of the PL stems from the coupling of exciting and emitted photons to the SPR excitation. A similar good agreement between the experimental and theoretical values (10^7) of enhancement factor was reported for gold nanorods[19] with the width 20 nm and aspect ratio 5.4. The strong PL enhancement (in 10^6 and 10^5 times) was reported also for spherical 30 and 12 nm copper nanoparticles.[21] Note that calculations show that the nanoparticle size at which the maximum of enhancement takes place and the relative intensity of B and P_l bands in spectrum depend on the constant A in Eq. (1). The decrease in A leads to the shift of maximum of enhancement to side of smaller sizes. We estimated for our calculations $A = 0.5$ based on the width of the diffuse reflectance spectra, Fig. 2. The width of the SPR band can be approximated as $\Gamma = \gamma_\infty + A\frac{v_F}{R}$, where γ_∞ is the bulk scattering rate for conduction electrons. The mismatch in the experimental (10 nm) and calculated (30 nm) size of silver nanoparticle for the maximum of the enhancement factor can therefore be explained by the choice of the A parameter. The A parameter contains both size and interface damping mechanisms[33,34] of the SPR excitation. In addition, the mismatch can be attributed to the simple local enhanced filed theory which we used to calculate the enhancement of the PL spectra.[28,29] A more sophisticated approach such as the many body theory[40] should remove this discrepancy and might be a subject of future theoretical investigations.

D. Influence of the excitation wavelength on the PL from silver nanoparticles

The excitation wavelength plays an important role in the PL spectra from silver nanoparticles. In this subsection, we present the experimental results on the dependence of the PL from silver nanoparticles on the excitation wavelength λ_{exc}. Figure 6(a) shows a behavior of the P_l band of the PL spectra

(a)

(b)
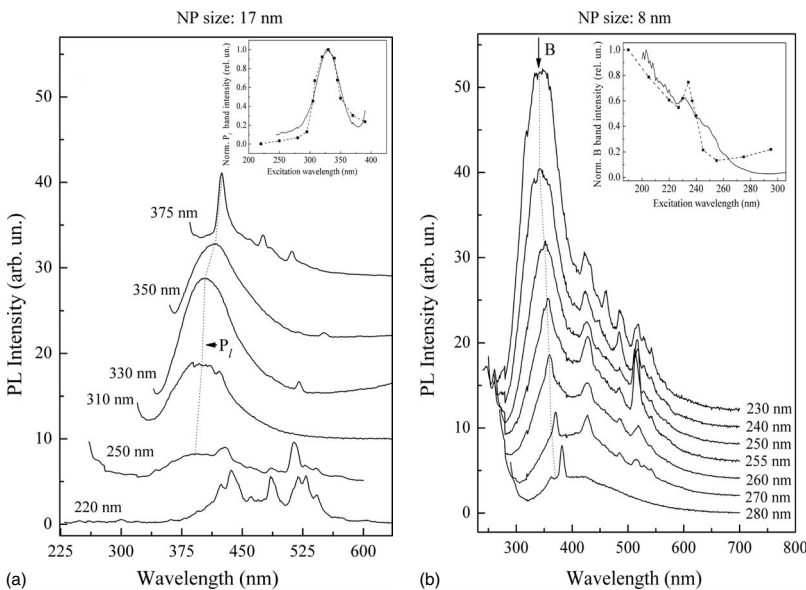
FIG. 6. Dependence of PL spectra of Ag/SiO$_2$ composites containing the silver nanoparticles with mean size 17 nm (a) and 8 nm (b) on excitation wavelength. Insets shows the normalized experimental (solid line) and calculated (squares and dashed line) excitation spectra of P$_l$ band (a) and B one (b).

from 17 nm silver nanoparticles as a function of the excitation wavelength and Fig. 6(b) depicts the B band of the PL spectra from 8 nm nanoparticles as a function of the excitation wavelength. Both bands in the PL spectra, namely, the interband recombination B and SPR radiative P_l band reveal a red shift of the PL maximum as the excitation wavelength increases as shown in Figs. 6(a) and 6(b).

The shift may be related to the size dependence of the SPR excitation in silver nanoparticles. Figure 2 shows the red shift of the DR scattering spectra caused by the SPR excitations in the nanoparticles. As the size of the particles decreases, we observe the red shift, which might be caused by the spill-out effect. We can expect the same dependence of both DR scattering P_s band and PL P_l on the size of the nanoparticles. Thus, as the size distribution of the silver nanoparticles is quite wide (standard deviation is 35–45%), the red shift of P_l band with increase in λ_{exc} can be the size distribution effect.

The red shift of interband recombination B band might be caused by the strong coupling of emitted photon of B band to SPR band. Such strong coupling might lead to transformation of the dispersion branch of the photon, i.e., some analog of "surface plasmon – photon" polaritons occurs. As a result of such coupling the states of photon and surface plasmon might attract to each other that would lead to the shift of the photon energy to SPR side. Since the SPR shifts to red side with increase in excitation wavelength [see Fig. 6(a)], this coupling has to lead to the red shift of the B band as the excitation wavelength increases. The similar shift of the interband PL band in copper nanoparticles from its position observed for bulk copper to side of SP resonance we observed recently.[20] In addition, our theoretical calculations of the PL spectra also indicate a synchronous shift of both bands, which additionally proves the "surface plasmon – photon" polariton coupling hypothesis.

Note that the intensities of both P_l and B bands depend on excitation wavelength as well. The intensity of the B band decreases monotonically as the excitation wavelength λ_{exc} increases with a slight local maximum at 230 nm. The dependence of intensity of P_l band on λ_{exc} is presented in the inset of Fig. 6(a). We can see that the most efficient excitation of surface-plasmon PL P_l band occurs at 330 nm that precisely coincides with the spectral position of the maximum of B band that corresponds to interband photoluminescence. That proves the fact of coupling of exciting and emitted photons to the SPR in nanoparticle. The agreement between the measured and calculated excitation spectra of P_l and B bands (see insets in Fig. 6) proves the validity of the theoretical model used to calculate the enhancement due to the coupling of exciting and emitted photons to SPR.

Finally, let us discuss the possibility of light emission from Ag-oxide clusters and ions and their contribution to the observed B and P_l bands of the PL spectra. First, we rule out the possibility of light emission from silver oxides. The B band was observed only in those in samples fabricated from xerogels with lower concentration of $AgNO_3$ and annealed in air atmosphere. If the emission of light was due to the silver oxides, then the B band would be observed with higher intensity in the samples with higher concentrations of $AgNO_3$ (samples with larger Ag nanoparticles). But this B band was not observed for the composites fabricated from the xerogels with larger initial concentration of $AgNO_3$, and so we conclude that the emission was not due to silver oxides. Moreover, if the emission of light was due to the silver oxides, the decrease in the $AgNO_3$ concentration would lead to smaller oxide nanoparticles and consequently to the blue shift of the band due to the quantum confinement effect well known for the semiconductor particles. Yet we observe the opposite red shift experimentally. Second, let us consider silver ions as possible origin of observed PL spectra. If the two B and P_l bands were from the silver ions emission, their intensities would increase with the increase in the concentration of $AgNO_3$ in initial xerogels, since the concentration of the ions in the host medium would increase as well. However, the opposite trend was observed both in the samples annealed in air and in hydrogen. If these bands were originating from ions, their spectral position would not change with the change in the concentration of $AgNO_3$ and excitation wavelength, whereas the shift of the B and P_l bands were observed with the change in both concentration and excitation wavelength.

IV. CONCLUSIONS

In conclusion, we studied experimentally the PL from spherical silver nanoparticles having the size in the range 8–30 nm embedded in a silica host medium. The two bands were observed in PL spectra of Ag nanoparticles. The high-energy band was observed in the samples containing 8 and 11 nm silver nanoparticles and was rationalized as the radiative recombination of the electrons in sp conduction band of silver with holes in d valence band. The low-energy band was observed in all the samples with the nanoparticles of sizes of 8–30 nm. The intensity of PL spectrum was found to increase when the nanoparticle size decreased. The quantum yield of the photoluminescence was found to be maximal for the smallest 8 nm silver nanoparticles and was estimated on the order of magnitude 10^{-2} that is in 10^8 times higher than in bulk silver. The theoretical calculations of the PL spectra from silver nanoparticles confirmed the size dependence of the PL spectra. The PL is enhanced by the local electric field due to enhancement of the exciting and emitted photons coupled to SPR in silver nanoparticle.

ACKNOWLEDGMENTS

[1] U. Kreibig and M. Vollmer, *Optical Properties of Metal Clusters* (Springer, Berlin, Heidelberg, 1995).

[2] C. F. Bohren and D. R. Huffman, *Absorption and scattering of light by small particle* (Wiley, New York, 1998).

[3] B. G. Ershov, E. Janata, A. Henglein, and A. Fojtik, J. Phys. Chem. **97**, 4589 (1993).

[4] A. Henglein, J. Phys. Chem. **97**, 5457 (1993).

[5] G. Schatz, M. Young, and R. Van Duyne, *Surface-Enhanced Raman Scattering, Physics and Applications* (Springer, Berlin, Heidelberg, New York, 2006), Vol. 103, p. 19.

[6] J. Kundu, F. Le, P. Nordlander, and N. Halas, Chem. Phys. Lett. **452**, 115 (2008).

[7] J. Wenger, P. Lenne, E. Popov, H. Rigneault, J. Dintinger, and T. Ebbesen, Opt. Express **13**, 7035 (2005).

[8] A. Whitney, R. Van Duyne, and F. Casadio, J. Raman Spectrosc. **37**, 993 (2006).

[9] D. Stuart, C. Yonzon, X. Zhang, O. Lyandres, N. Shah, M. Glucksberg, J. Walsh, and R. Van Duyne, Anal. Chem. **77**, 4013 (2005).

[10] J. Hulteen, M. Young, and R. Van Duyne, Langmuir **22**, 10354 (2006).

[11] A. P. Zhang, J. Z. Zhang, and Y. Fang, J. Lumin. **128**, 1635 (2008).

[12] H. Mertens and A. Polman, Appl. Phys. Lett. **89**, 211107 (2006).

[13] S. W. Chen, R. S. Ingram, M. J. Hostetler, J. J. Pietron, R. W. Murray, T. G. Schaaff, J. T. Khoury, M. M. Alvarez, and R. L. Whetten, Science **280**, 2098 (1998).

[14] R. S. Ingram, M. J. Hostetler, R. W. Murray, T. G. Schaaff, J. T. Khoury, R. L. Whetten, T. P. Bigioni, D. K. Guthrie, and P. N. First, J. Am. Chem. Soc. **119**, 9279 (1997).

[15] P. Apell, R. Monreal, and S. Lundqvist, Phys. Scr. **38**, 174 (1988).

[16] D. J. Whittle and E. Burstein, Bull. Am. Phys. Soc. **26**, 777 (1981).

[17] A. Mooradian, Phys. Rev. Lett. **22**, 185 (1969).

[18] J. P. Wilcoxon, J. E. Martin, F. Parsapour, B. Wiedenman, and D. F. Kelley, J. Chem. Phys. **108**, 9137 (1998).

[19] M. B. Mohamed, V. Volkov, S. Link, and M. A. El-Sayed, Chem. Phys. Lett. **317**, 517 (2000).

[20] O. A. Yeshchenko, I. M. Dmitruk, A. M. Dmytruk, and A. A. Alexeenko, Mater. Sci. Eng., B **137**, 247 (2007).

[21] Q. Darugar, W. Qian, M. A. El-Sayed, and M. P. Pileni, J. Phys. Chem. B **110**, 143 (2006).

[22] D. Basak, S. Karan, and B. Mallik, Chem. Phys. Lett. **420**, 115 (2006).

[23] M. Fleischmann, P. J. Hendra, and A. J. McQuillan, Chem. Phys. Lett. **26**, 163 (1974).

[24] Y. Fang, N. H. Seong, and D. D. Dlott, Science **321**, 388 (2008).

[25] E. Ozbay, Science **311**, 189 (2006).

[26] O. L. Muskens, V. Giannini, J. A. Sanchez-Gil, and J. G. Rivas, Nano Lett. **7**, 2871 (2007).

[27] Y. X. Zhang, K. Aslan, M. J. R. Previte, and C. D. Geddes, Appl. Phys. Lett. **90**, 173116 (2007).

[28] G. T. Boyd, T. Rasing, J. R. R. Leite, and Y. R. Shen, Phys. Rev. B **30**, 519 (1984).

[29] G. T. Boyd, Z. H. Yu, and Y. R. Shen, Phys. Rev. B **33**, 7923 (1986).

[30] V. S. Gurin, A. A. Alexeenko, K. V. Yumashev, R. Prokoshin, S. A. Zolotovskaya, and G. A. Zhavnerko, Mater. Sci. Eng., C **23**, 1063 (2003).

[31] O. A. Yeshchenko, I. M. Dmitruk, A. A. Alexeenko, and A. M. Dmytruk, Phys. Rev. B **75**, 085434 (2007).

[32] P. B. Johnson and R. W. Christy, Phys. Rev. B **6**, 4370 (1972).

[33] A. Pinchuk, U. Kreibig, and A. Hilger, Surf. Sci. **557**, 269 (2004).

[34] A. Pinchuk and U. Kreibig, New J. Phys. **5**, 151 (2003).

[35] N. Ashcroft and D. Mermin, *Solid Sate Physics* (Brooks/Cole, Belmont, 1976).

[36] F. T. Xie, H. Y. Bie, L. M. Duan, G. H. Li, X. Zhang, and J. Q. Xu, J. Solid State Chem. **178**, 2858 (2005).

[37] A. V. Akimov, A. Mukherjee, C. L. Yu, D. E. Chang, A. S. Zibrov, P. R. Hemmer, H. Park, and M. D. Lukin, Nature (London) **450**, 402 (2007).

[38] V. A. Kosobukin, Phys. Lett. A **160**, 584 (1991).

[39] S. M. Nie and S. R. Emery, Science **275**, 1102 (1997).

[40] F. Gallagher III, W. Beasley, and C. Bohren, Bull. Am. Meteorol. Soc. **77**, 2889 (1996).